Research Article

Krzysztof Przybył*, Katarzyna Samborska, Aleksandra Jedlińska, Krzysztof Koszela, Hanna Maria Baranowska, Łukasz Masewicz, and Przemysław Łukasz Kowalczewski

The application of convolutional neural networks, LF-NMR, and texture for microparticle analysis in assessing the quality of fruit powders: Case study – blackcurrant powders

https://doi.org/10.1515/rams-2025-0132
received March 12, 2024; accepted July 08, 2025

Abstract: It can be observed that dynamic developments in artificial intelligence contributing to the evolution of existing techniques used in food research. Currently, innovative methods are being sought to support unit processes such as food drying, while at the same time monitoring quality and extending their shelf life. The development of innovative technology using convolutional neural networks (CNNs) to assess the quality of fruit powders seems highly desirable. This will translate into obtaining homogeneous batches of powders based on the specific morphological structure of the obtained microparticles. The research aims to apply convolutional networks to assess the quality, consistency, and homogeneity of blackcurrant powders supported by comparative physical methods of low-field nuclear magnetic resonance (LF-NMR) and texture analysis. The results show that maltodextrin, inulin, whey milk proteins, microcrystalline cellulose, and gum arabic are effective carriers when identifying morphological structure using CNNs. The use of CNNs, texture analysis, and the effect of LF-NMR relaxation time together with statistical elaboration shows that maltodextrin as well as milk whey proteins in combination with inulin achieve the most favorable results. The best results were obtained for a sample containing 50% maltodextrin and 50% maltodextrin (MD50-MD70). The CNN model for this combination had the lowest mean squared error in the test set at 2.5741×10^{-4}, confirming its high performance in the classification of blackcurrant powder microstructures.

Keywords: convolutional neural networks, low-field nuclear magnetic resonance, texture analysis, scanning electron microscopy, fruit powders, blackcurrant

*** Corresponding author: Krzysztof Przybył,** Department of Dairy and Process Engineering, Poznań University of Life Sciences, 31 Wojska Polskiego St., 60-624, Poznań, Poland; Department of Biosystems Engineering, Poznań University of Life Sciences, 50 Wojska Polskiego St., 60-627, Poznan, Poland, e-mail: krzysztof.przybyl@up.poznan.pl
Katarzyna Samborska: Institute of Food Sciences, Warsaw University of Life Sciences WULS-SGGW, 159c Nowoursynowska St., 02-787, Warsaw, Poland, e-mail: katarzyna_samborska@sggw.edu.pl
Aleksandra Jedlińska: Institute of Food Sciences, Warsaw University of Life Sciences WULS-SGGW, 159c Nowoursynowska St., 02-787, Warsaw, Poland, e-mail: aleksandra_jedlinska@sggw.edu.pl
Krzysztof Koszela: Department of Biosystems Engineering, Poznań University of Life Sciences, 50 Wojska Polskiego St., 60-627, Poznan, Poland, e-mail: koszela@up.poznan.pl
Hanna Maria Baranowska: Department of Physics and Biophysics, Poznań University of Life Sciences, 28 Wojska Polskiego St., 60-637, Poznań, Poland, e-mail: hanna.baranowska@up.poznan.pl
Łukasz Masewicz: Department of Physics and Biophysics, Poznań University of Life Sciences, 28 Wojska Polskiego St., 60-637, Poznań, Poland, e-mail: lukasz.masewicz@up.poznan.pl
Przemysław Łukasz Kowalczewski: Collegium Medicum, Andrzej Frycz Modrzewski Krakow University, 1 Gustawa Herlinga-Grudzińskiego St., 30-705, Kraków, Poland; Department of Food Technology of Plant Origin, Poznań University of Life Sciences, 60-624, Poznań, Poland, e-mail: przemyslaw.kowalczewski@up.poznan.pl

1 Introduction

Following the development of technology, advanced techniques have been introduced to ensure sustainability, safety, and quality in the production and distribution of food [1]. Food preservation is achieved through traditional processes such as drying, conserving, pasteurization, or freezing [2–4]. Artificial intelligence is becoming a key aspect in the optimization of these processes [5,6]. Different methods of machine learning, including deep learning, will primarily allow to minimize the risk of inefficiently obtained food products, which translates into the reduction of waste of the final product obtained. In the age of Industry 4.0 and 5.0 in food production and processing, to use of advanced methods like image analysis, automation, robotics, artificial

intelligence, and data analysis is becoming more effective and improves the quality condition as well as the reproducibility of the obtained food products [4,7–10]. Advanced machine and deep learning techniques allow more efficient management of products, water, and energy in the process of obtaining and processing the above [11]. In addition, the use of machine and deep learning algorithms allows to accurately monitor and control the quality condition of food products at various stages of food processing [12,13].

Nowadays, companies try to offer the market as natural a colorant as possible. As a result of low-temperature spray drying, blackcurrant powders [14–16] were obtained in the research. Fruit powders add flavor and functionality to various products such as teas, jellies, puddings, instant soups, instant drinks, all dairy products, dietary supplements, confectionery, pharmaceutical preparations, *etc*. In fact, proper preservation of blackcurrant powder will maintain the content of bioactive compounds in the resulting food products and preserve their quality coefficient. It is worth knowing that exposure to high temperatures causes changes in the nutritional value of powders. Deterioration of the quality of products as a result of their storage at room temperature causes degradation of compounds, including the oxidation of vitamins. Effective yet low-energy methods are being sought to prevent the degradation of compounds.

Recent results show that there are few works using deep learning solutions in the context of spray drying [12]. This is due to the fact that spray drying is a complicated process for obtaining fruit powders. The process of spray drying carries the risk of not obtaining homogeneous powders, giving the correct morphological structure to the powder microparticles, and thus obtaining the right quality of the final product. For this reason, it is very important, in addition to the established drying parameters (inlet and outlet air temperatures, determination of air velocity flux and humidity), to adjust the way of controlling the morphological structure of powder microparticles in order to minimize the loss of their quality [17–19]. In another recent research, an attempt was made to use traditional artificial neural network (ANN) methods and convolutional neural networks (CNNs), to identify raspberry powders that differ in the amount and type of polysaccharides [20]. The aim of this work was to develop optimal multi-layer perceptron network and CNNs with optimal classification performance. The new methods used are the result of technological advances, acquired knowledge, as well as experience. The new developments use advanced algorithms, neural network models, and data processing techniques that contribute to better performance and capabilities in analysis, prediction, and decision-making problems in the field of machine and deep learning.

This research aims to fill a gap in the analysis of food quality and preservation by evaluating the morphological structure of fruit powder microparticles using CNNs, which are among the most advanced methods of artificial intelligence, specialized low-field nuclear magnetic resonance (LF-NMR) and instrumental texture analysis [21–24]. The morphology of microparticles can be captured using digital images, allowing for faster analysis of large amount of image data. CNN will effectively analyze individual areas of powder microparticles contained in the image, which will serve as input data, and generate new tensors from them. The application of deep learning based on CNN will determine an effective algorithm for image classification due to the presence of repeated, recognizable, and similar patterns in the image [25]. The image pattern will determine the state of morphological structure for each variant of blackcurrant powder. When determining the pattern, a description characterizing the shape of the microparticle found in the image, the height of the image, the width of the image, and the depth as the number of dimensions of the color space [26] will be used as the input tensor of the network. As part of the comparative analysis of the structure of blackcurrant powders, the use of a specialized LF-NMR method allows us to effectively understand the research samples obtained by analyzing the molecular structure of blackcurrant powders. In addition, the instrumental texture was used in the study to provide a link in the effective identification of blackcurrant powders. LF-NMR and texture analyses combined with CNN provide complete information on the quality, properties, and structure of the analyzed powders.

2 Materials and methods

2.1 Preparation of a solution from blackcurrant concentrate, taking into account the amount and content of the selected carrier, and performing low-temperature spray drying

As part of the implementation of the scientific activity, concentrated blackcurrant juice (blackcurrant concentrate) with a density of 67°Brix and a color coefficient of 2.352 (E520/E420) was purchased in the amount of 5 kg obtained from a batch of 250 kg of this product from the company Białuty Sp. z o.o and carriers such as maltodextrin

(MD; Hortimex), gum arabic (GA; Hortimex), inulin (IN; Hortimex), milk whey protein (WPC; Mlekovita), fiber (F; Hortimex), and microcrystalline cellulose (C; Hortimex). Preparation of solutions was done by mixing blackcurrant concentrate with the appropriate amount of water and carriers. Twelve solution variants were prepared (Table 1), which differed in the type and proportion of carrier. The proportion of carriers in the solution was 30 and 50% solids, respectively. The solutions were prepared by mixing the concentrate with the appropriate amount of water and carrier, and then dried in batches of 600 g.

The prepared solutions were dried in a laboratory dryer at an inlet air temperature of 80°C and outlet air temperature of 50°C. During the drying process, the humidity of the air was 0.5 g·cm^{-3}. The feed flow rate was 0.3 mL·s^{-1}. As a result of low-temperature drying, blackcurrant powders were obtained.

2.2 Physical analysis of blackcurrant powders (LF-NMR and instrumental texture)

The analysis was carried out in order to characterize the properties of blackcurrant powders, which allows for effective assessment of their quality. Instrumental texture measurement of blackcurrant powders was carried out using a TA.XTplus Texture Analyzer (Stable Micro Systems, UK) with an SMS P36R attachment. A calibration of the attachment height of 110 mm was performed, 40% compression for samples up to 25 mL was taken into account. The sample weight was 58 ± 0.1 g. For each test variant, eight replicates were performed. A total of 96 teaching cases were obtained in the numerical dataset.

Table 1: Names of the blackcurrant powders were determined by their dependence on the type and proportion of the carrier

Type of carrier	The ratio of blackcurrant concentrate to carrier solids	
	50:50	70:30
Arabic gum (GA)	GA50	GA70
Maltodextrin (MD)	MD50	MD70
Inulin (IN)	IN50	IN70
Whey protein (W)	W50	W70
Fiber (F)	F50	F70
Microcrystalline cellulose (C)	C50	C70

As an additional research, a comparative measurement was performed by measuring the blackcurrant powder variants by LF-NMR. Samples of the analyzed powders were placed in 7 mm diameter measuring tubes. The tubes were sealed with Parafilm®. The volume of the samples was 770 mm^3.

The spin–lattice T_1 relaxation times were measured using pulse NMR spectrometer PS15T operating at 15 MHz (Ellab, Poznań, Poland). The inversion-recovery (180°–TI–90°–TR) pulse sequence was applied [27,28]. The 90° radio pulse (RF) pulse was from 2.2 to 2.6 ms. The distance inversion time (TI) between RF pulses was changed from 0.2 to 100 ms, the repetition time repetition time was 15 s. Each time, 32 free induction decay (FID) signals and from 38 to 54 points from each FID signal were collected. Five accumulations of NMR signals were applied each time.

Calculations of the T_1 relaxation time values were performed with CracSpin software (Jagiellonian University, Cracow, Poland) [29] using a "spin grouping" approach. The accuracy of the relaxation parameters was determined, and standard deviations were calculated. The recovery of the magnetization was described by the equation given below [29]:

$$M_z(\mathrm{TI}) = M_0\left[1 - 2e\frac{-\mathrm{TI}}{T_1}\right], \quad (1)$$

where M_z(TI) is the actual magnetization value and M_0 is the equilibrium magnetization value.

Monoexponential magnetization recovery, observed in this study, indicated that the system relaxed within one TI spin–lattice relaxation time. The measurements were performed in controlled temperature at 20.0 ± 0.5°C. As a result, 12 cases of each research variant were acquired.

2.3 Microscope image acquisition and processing

The next step required preparing blackcurrant powder samples for morphological structure determination using a scanning electron microscope (SEM). The samples were attached to the sample section with double-sided adhesive tape and cathodically sputtered with gold. The instrument was calibrated with a secondary electron detector before testing. The working distance of the detector from the samples was 10 mm inside (WD = 10 mm). The accelerating voltage for each sample was 12.82 kV. There were 35 repetitions in the form of microscope photographs for each variant of blackcurrant powders. Photographs of microparticles were obtained at 500 times magnification at a scale of 100 µm (a total of 420 microscope images).

After the problem was formulated in machine learning, preprocessing of microscope images with a resolution of 2,048 × 1,576 (the original images) and their format with a.TIFF extension was carried out. For this purpose, the free Python Imaging Library (PIL) was used [30,31]. The PIL library is one of the most popular tools for image processing using the Python language. The PIL library allows for automated yet fast image conversion, point transformations, batch processing, filtering, bit depth transformation, and changing the color space of images. In technical terms, the goal of image processing is to skillfully acquire a pattern, adjust filtering, transformations, storage format changes, and image resolution for better quality of the resulting image. In view of the above, image processing seems to be important in the field of machine learning in the aspect of computer vision to improve the quality and extract the necessary information from the established pattern of images.

In the first step of the study, primary images with a.TIFF extension were converted to secondary images with a.jpg extension. The converted images were saved under a new name. The next step was to do segmentation of the images. The number of segments along the *x*-axis and *y*-axis was calculated, which made it possible to perform cropping of the secondary images by the indicated step relative to the *x*- and *y*-axis parameters. In order to automate the process, the batch cropping of these images was performed again using the PIL library. The result was 1,400 × 1,400 resolution secondary images, the aim of which was to obtain a consistent view of the data. The final step was to perform a point transformation on the images. The segmented secondary images were subjected to 90°, 180°, and 270° transformations and stored in the output catalog. As a result of data pre-processing, 105 digital images corresponding to the learning set were obtained for each research variant of blackcurrant powders. The purpose of pre-processing of secondary images obtained by image processing, in addition to the qualitative measures mentioned above, becomes the normalization of the input data in the learning set. The rescaling of the pixel values of the images in the image analysis will improve the quality of learning the designed neural models in the machine learning process.

2.4 Design and learning of convolutional networks

This step required the formulation of the variables in the sets and the selection of a machine-learning algorithm to design the model and carry out the learning process to obtain an adequate determination index of blackcurrant powders. Two learning and test sets were prepared for each research variant. An important step in preparing the sets is to determine the split between the learning set and the test set. In computer vision machine learning, the split is assumed to be 60:40, 70:30, or 80:20 [32,33]. In the work averaging, the division of the sets was made at a ratio of 75:25. The learning set contained 105 images processed through data pre-processing. The test set contained 35 microscope images with a fixed resolution of 1,400 × 1,400, which were not in the learning set. In the test samples, using microscope images (SEM), 36 learning sets were finally created, which represented combinations with the lowest (30%) (total n = 15) and highest (50%) (total n = 15) proportion of the selected type (total n = 6) of carrier in the blackcurrant solution.

The design of convolutional networks was performed using 36 variants of blackcurrant powder sets. The goal of this stage was to develop CNNs. In the design of CNNs using the Tensorflow and KERAS libraries, the sequential model is used, which is one of the simplest and most popular ways of building models in the library [34]. The sequential model is a linear application of layers, meaning that each layer has one input and exactly one output, and data flow between convolutional layers, activation function, and pooling layers [35]. The structure of the designed convolutional networks for each learning set included: convolution layers (Convolution) to determine the size of the input tensor, max pooling layers (Max-Pooling) to reduce the size of the input tensor, flattening layer (Flatten) to transform the image to a vector, and dense layers as densely connected. In research the sequential CNN model consisted of eight layers: convolutional layers (Conv2D) and maximum pooling layers (MaxPooling2D). The CNN model also included a flattening layer to transform the multidimensional input data (image pixels of blackcurrant powder) into a one-dimensional vector. The model also used a dense layer of 288 neurons, meaning that each neuron was connected to the input of the previous layer. This layer used the ReLU activation function, which introduces non-linearity into the network, allowing the model to better represent the complexity of the data. The output layer consisted of a neuron and a sigmoidal activation function, which transformed the result into a value between 0 and 1, accurately representing the blackcurrant varieties. The structure is shown in Figure 1. The initialization of the CNN used a loss function of the “binary_crossentropy” type, applied to this research as binary classification problem. The “adam” learning algorithm was used, which is the most popular and probably the most efficient optimization algorithm for updating weights during CNN learning [36–38].

An essential step in the design of suitable neural models for microscopic images identification was the analysis between overfitting and underfitting. In order to avoid over-fitting of the CNN model to the learning set and also to effectively use these networks in image recognition, a scaling of the data was performed [39]. This involved the creation of additional convolutional layers for the input tensor, resulting in a balance between the fit and generalization ability of the CNN models.

2.5 Statistical analysis

The research article presents results using analysis of variance (ANOVA) [40,41] and principal component analysis () [42–44] methods. A Tukey test was applied for each sample with a significance level of $p = 0.05$ [45,46]. Python and Statistica 13.3 were used to perform statistical analysis. Using the Tukey test after ANOVA, differences between blackcurrant powder variants were statistically determined in Python. The scipy and scikit-learn libraries were used within the Python environment [47,48]. For the PCA method, relationships between textural variables were identified in Statistica 13.3 (TIBCO Software Inc., Palo Alto, CA, USA).

3 Results

3.1 Preparation of a solution from blackcurrant concentrate, taking into account the amount and content of the selected carrier, and performing low-temperature spray drying

As a result of dehumidified air-assisted drying, blackcurrant powders were obtained according to the procedure of Przybyl *et al.* [15]. Table 1 shows different combinations of carriers, *i.e.*, gum arabic, maltodextrin, inulin, whey milk proteins, fiber, microcrystalline cellulose, along with their specific proportion in solution, *i.e.*, the smallest (30% content) and the largest (50% content). As a result, 12 variants of blackcurrant powders were obtained.

3.2 Physical analysis of blackcurrant powders (LF-NMR and instrumental texture)

According to statistical analyses using the Tukey test, PCA, and correlation methods, the relationships between

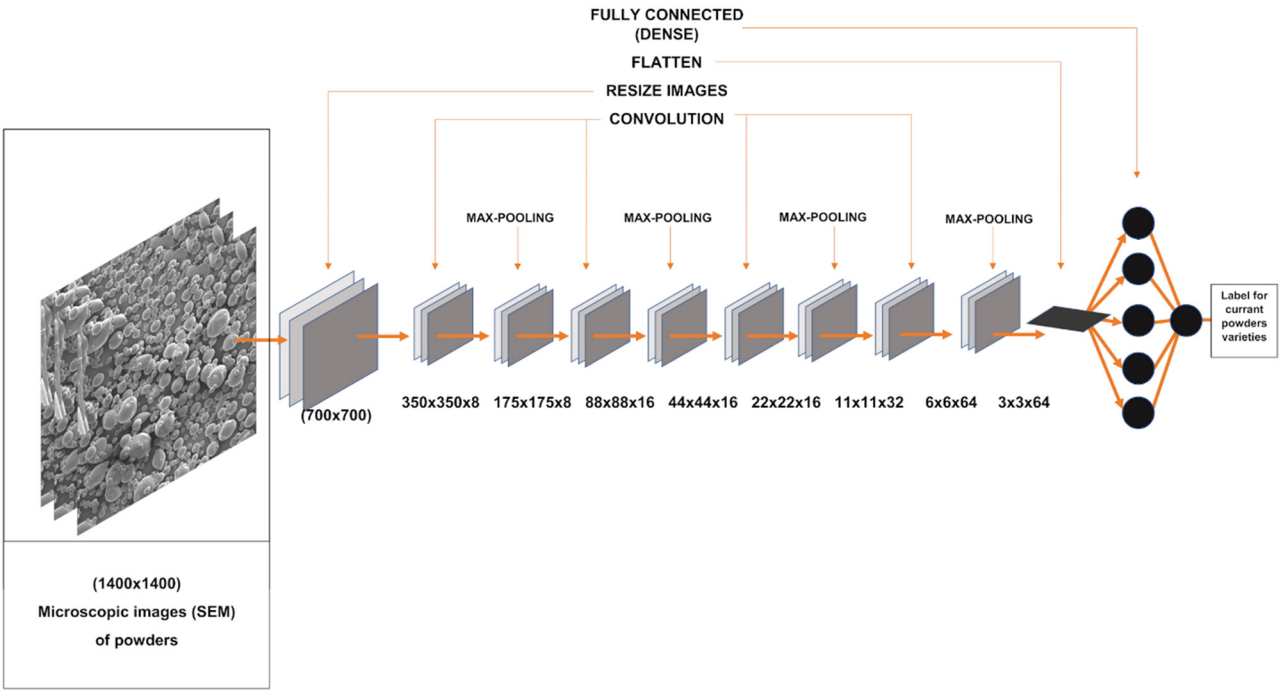

Figure 1: CNN model structure in blackcurrant powders.

textural parameters and T_1 relaxation time were compared using the LF-NMR method. T_1 relaxation time and textural coefficients in blackcurrant powders made it possible to assess their quality, porosity, homogeneity, and the degree of structure in which individual microparticles are bound together. The correlation between the textural variables is intended to show the degree of interrelatedness (Figure 2). Table 2 shows the textural coefficients and T_1 relaxation time from the LF-NMR method. It turned out that maltodextrin (50% share) and milk whey proteins (30% carrier content) were the most statistically significantly different from the other test variants of blackcurrant powders. The average values shown in Table 2 for each homogeneous group showed that maltodextrin and whey proteins are significantly different from the remaining coefficients.

In the study of textual analysis, cohesiveness, springiness, chewiness, gumminess, resilience, force (Force_1), hardness, and adhesiveness were determined for blackcurrant powders. Maltodextrin showed the lowest Force_1 at 4547.55, and this translates into regularity, linearity in the microparticle structure of this blackcurrant powder variant. As Force_1 increases, their level of texture in blackcurrant powders changes, causing irregularities in the structure or increased inter-particle spaces. In the case of the hardness coefficient, for which the qualitative analysis of the powders affects their degree of granularity [49] was also statistically shown that the maltodextrin carrier was one of the three to achieve the lowest value at 8885.17 relative to the other test variants. The lowest hardness of the powders was shown for the milk whey protein carrier (6603.19) and the highest hardness was achieved by the blackcurrant powder variant with gum arabic (32912.67). Blackcurrant powders with a higher hardness coefficient may tend to form the so-called clumps in the morphological structure of microparticles [49].

Moreover, the higher the hardness of coefficient, the more favorable the flow, spreadability, and stability of powders. Adhesiveness, on the other hand, has a significant effect on the solubility of powders. The higher the adhesiveness index, the more difficult it is for the carrier to dissolve in solutions. The results in Table 2 relating to adhesiveness statistically show that whey protein and microcrystalline cellulose have the lowest solubility index in food products. In the case of springiness or resilience, which determines the ability of powders to return to their original shape, the different research variants do not differ statistically in their values. Nevertheless, their low content indicates lower elasticity, which means that they do not return to their original shape. Cohesiveness as the primary determinant of intermolecular bonding of powders from the point of view of microparticle structure, has an impact on their cohesion [50,51]. Within the individual variants of powders, the cohesion index was determined to be significantly low. This means that blackcurrant powders have a lower tendency to form agglomerates and lumps [52]. Low cohesiveness significantly affects scattering and the microparticles will allow them to separate more efficiently.

Proper storage of these powders is essential. In the case of the coefficient of gumminess, which is responsible

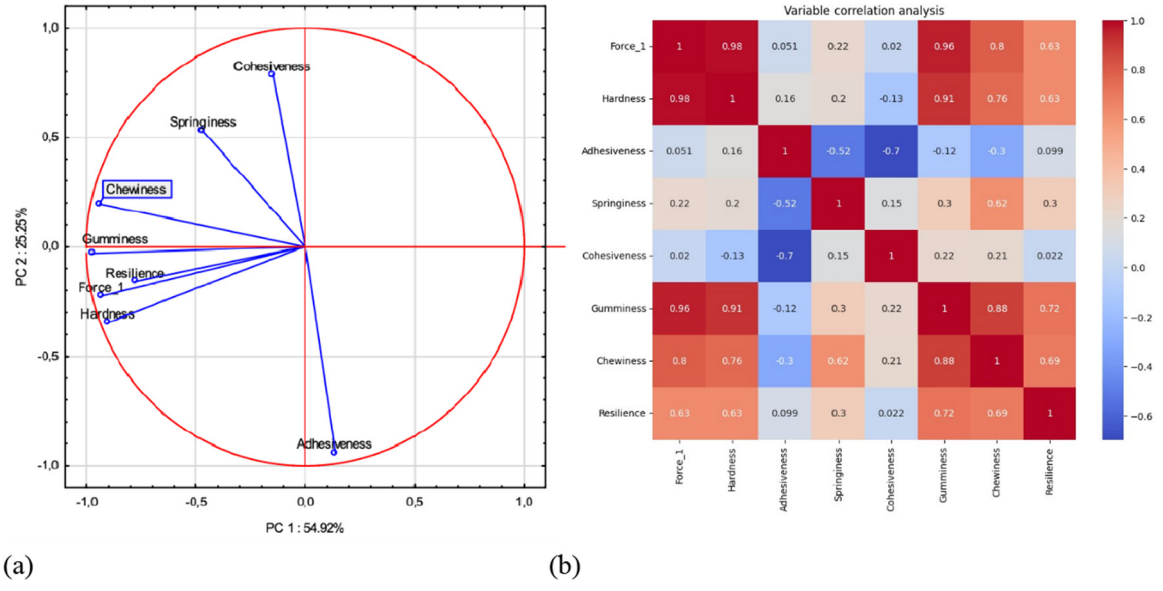

Figure 2: PCA (a) combined with correlation (b) of textural variables.

Table 2: Texture coefficients and spin–lattice relaxation times of blackcurrant powders containing 50% and 30% carrier gum arabic (GA), inulin (IN), maltodextrin (MD), whey protein (W), fiber (F), and microcrystalline cellulose (C) by dehumidified air-assisted spray drying

	T_1	Force	Hardness	Adhesiveness	Springiness
MD50	70.66 ± 2.46	4547.55 ± 538.24a	8885.17 ± 1356.42ab	−9.87 ± 9.93b	0.57 ± 0.24ba
MD70	68.20 ± 3.58	5435.31 ± 1614.63ab	11007.98 ± 3328.79ab	−3.63 ± 3.64b	0.49 ± 0.31ba
GA50	115.41 ± 10.80	18160.68 ± 3804.28d	32912.67 ± 6195.51d	−9.28 ± 4.81b	0.74 ± 0.22b
GA70	71.95 ± 5.79	10733.51 ± 4385.58c	20781.50 ± 7769.08c	−4.37 ± 2.39b	0.47 ± 0.09ba
IN50	93.43 ± 10.55	5628.67 ± 1480.43ab	10932.30 ± 3003.33ab	−5.65 ± 7.16b	0.45 ± 0.35ba
IN70	58.31 ± 6.26	6387.79 ± 2638.03ab	11788.26 ± 4491.27ab	−1.87 ± 1.49b	0.35 ± 0.15a
C50	53.32 ± 4.50	5672.24 ± 1161.70ab	11167.43 ± 2188.69ab	−5.53 ± 1.12b	0.36 ± 0.15a
C70	93.29 ± 3.30	5997.64 ± 1814.92ab	12244.32 ± 3348.27ab	−9.75 ± 3.66b	0.78 ± 0.33b
F50	44.76 ± 5.26	9401.71 ± 3930.57bc	16668.08 ± 8541.36bc	−26.90 ± 10.57a	0.82 ± 0.21b
F70	86.69 ± 2.90	6378.40 ± 1288.15ab	11734.90 ± 2612.61ab	−3.65 ± 2.66b	0.49 ± 0.20ba
W50	74.97 ± 8.30	5890.29 ± 2272.78ab	8742.09 ± 4249.09a	−23.40 ± 10.14a	0.47 ± 0.17ba
W70	71.19 ± 5.30	4615.75 ± 1277.42a	6603.19 ± 3164.72a	−23.06 ± 7.20a	0.50 ± 0.13ba

	Cohesiveness	Gumminess	Chewiness	Resilience
MD50	0.13 ± 0.02a	1181.10 ± 186.94a	680.13 ± 334.10a	0.12 ± 0.01ba
MD70	0.14 ± 0.01ab	1579.05 ± 503.14a	747.83 ± 527.33a	0.14 ± 0.01bc
GA50	0.21 ± 0.01abc	6816.16 ± 1201.99c	5161.88 ± 2049.06c	0.23 ± 0.02g
GA70	0.15 ± 0.01ab	3127.73 ± 1019.03b	1444.85 ± 552.23a	0.15 ± 0.02cd
IN50	0.13 ± 0.01a	1387.29 ± 361.55a	657.45 ± 614.32a	0.12 ± 0.01ba
IN70	0.15 ± 0.02ab	1796.63 ± 828.21a	596.40 ± 270.52a	0.13 ± 0.01bac
C50	0.14 ± 0.01ab	1581.53 ± 289.09a	555.18 ± 180.14a	0.13 ± 0.01bac
C70	0.14 ± 0.01ab	1757.94 ± 621.35a	1470.84 ± 874.29ab	0.14 ± 0.01bc
F50	0.23 ± 0.04bcd	3471.43 ± 958.24b	2778.30 ± 806.74b	0.18 ± 0.03de
F70	0.19 ± 0.02ab	2268.24 ± 542.67ab	1055.32 ± 314.18a	0.19 ± 0.02e
W50	0.29 ± 0.14cd	2356.36 ± 986.97ab	1242.89 ± 650.15a	0.12 ± 0.02ba
W70	0.30 ± 0.10d	1734.71 ± 397.17a	868.41 ± 337.69a	0.10 ± 0.01a

a–g: the differences between mean values with the same letter in columns without column T_1 were statistically significant ($p < 0.05$). Column T_1 corresponds to the resulting values using the LF-NMR method.

for the elasticity of the powders, it was shown that the highest elasticity, viscosity, was achieved by the powder variant with arabic gum (GA50) with a value of 6816.16 and the lowest with maltodextrin (MD50) with a value of 1181.10. Chewiness in instrumental texture refers to the degree of difficulty in breaking and chewing the food product. Very low chewiness was again achieved by maltodextrin and the highest value by arabic gum.

As part of the comparative analysis between the instrumental texture results, the relationships of relaxation times were determined [24,53], which illustrated the molecular movements of water in blackcurrant powders. The LF-NMR method made it possible to find a specific range of temperatures at which the formation of lattice nodes occurs for the different variants of blackcurrant powders. The longest T_1 relaxation time by LF-NMR was achieved by the variant with gum arabic carrier (GA50), while the shortest T_1 was achieved by the variant with fiber (F50). In practical terms, this means that the longer the T_1 relaxation time obtained with LF-NMR, the more ordered the structure of the blackcurrant powder microparticles becomes (a more solid-body structure).

The correlation and PCA result (Figure 2a and b) when evaluating the dimensionality reduction of the data and attempting to extract significant data, it can be found that cohesiveness is strongly negatively correlated with adhesiveness giving a correlation coefficient of $R^2 = -0.7$. This means that the strong negative correlation between cohesiveness and adhesiveness determines the greatest variability between each other. The principal component of PC1 reflects the direction in which there is the greatest correlation between cohesiveness and adhesiveness. In the case of PC2, this measure shows the opposite direction of the relationship between these data. It was observed that Force_1 shows a strong correlation between hardness $R^2 = 0.98$ and resilience $R^2 = 0.96$. This is due to the fact that the strong correlation between these variables affects the variability of the principal components. The variable Force_1, which determines the effect of the texture on the morphological structure of blackcurrant powder microparticles, responds to the other variables hardness and resilience

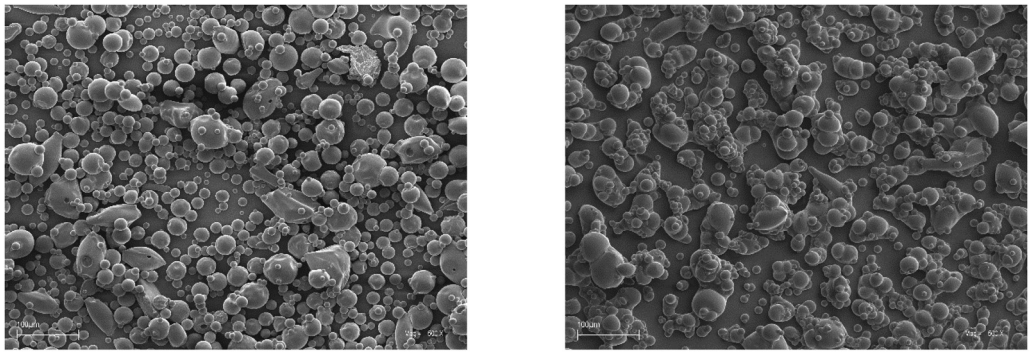

C50
(a)

C70
(b)

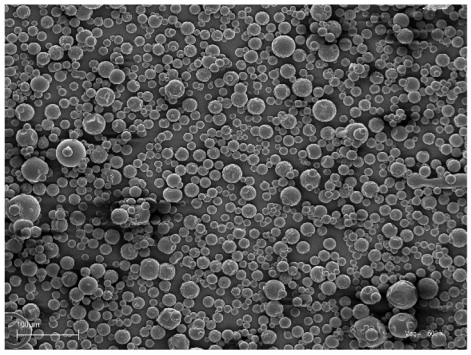

MD50
(c)

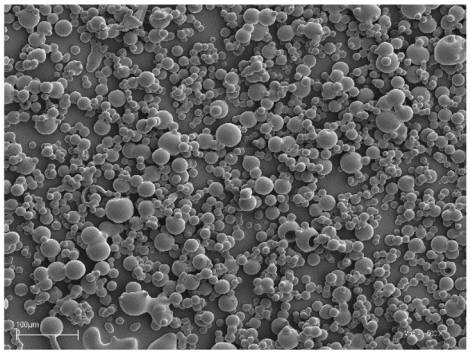

MD70
(d)

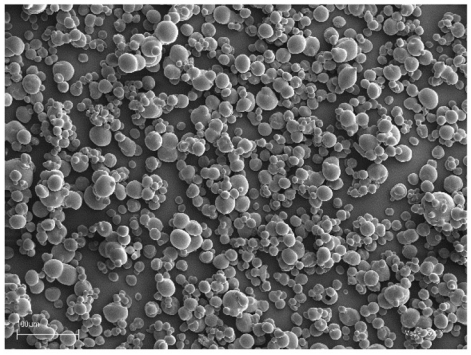

W50
(e)

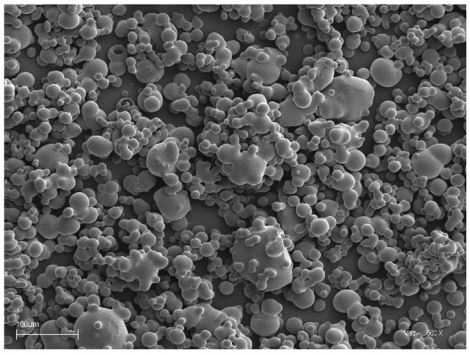

W70
(f)

Figure 3: Microparticles from 12 variants of blackcurrant powders containing 50%,and 30% carrier microcrystalline cellulose (C) (a) and (b), maltodextrin (MD) (c) and (d), whey protein (W) (e) and (f), fiber (F) (g) and (h), gum arabic (GA) (i) and (j), and inulin (IN) (k) and (l) which were isolated from microscope image (SEM).

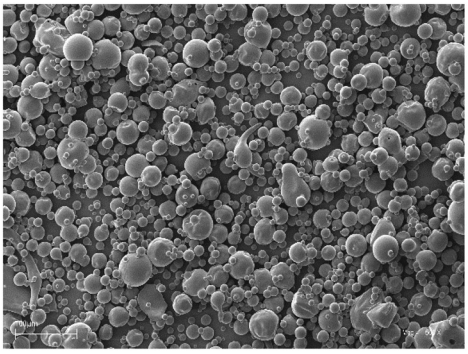

F50
(g)

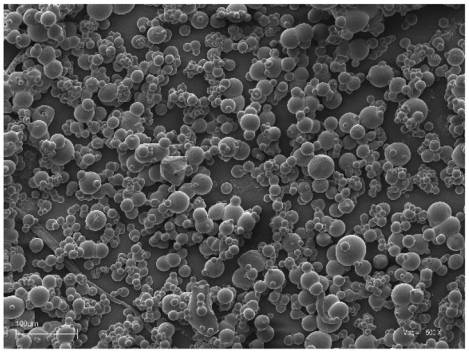

F70
(h)

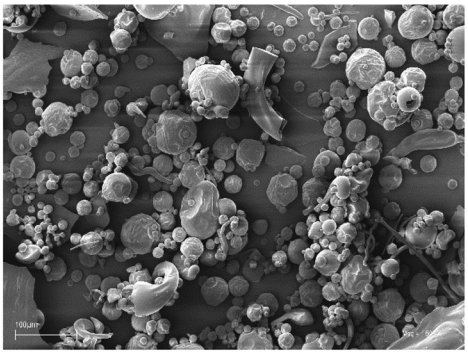

GA50
(i)

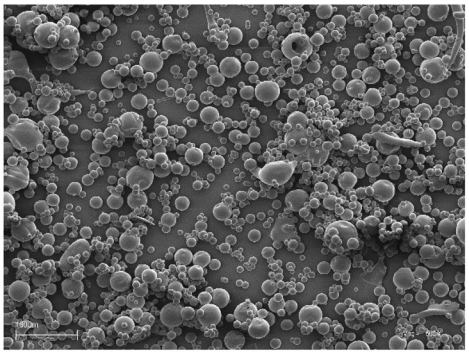

GA70
(j)

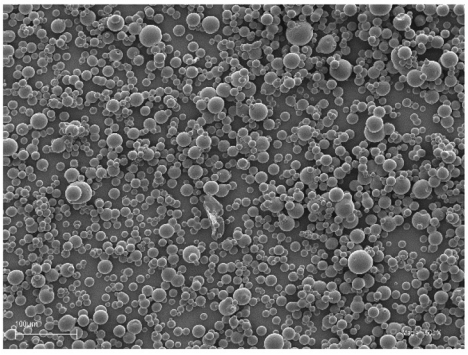

IN50
(k)

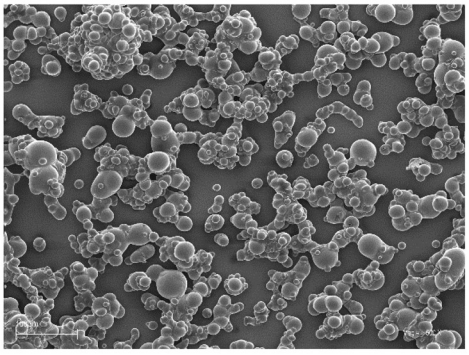

IN70
(l)

Figure 3: (*Continued*)

by determining, among other things, the variability of microparticle shape. Considering the aforementioned variable hardness shows a strong correlation with the variable gumminess (R^2 = 0.91), and the variable gumminess shows a strong correlation with chewiness (R^2 = 0.88). This expresses common information about the powder microparticle that significantly influences the principal components in the PCA.

3.3 Microscope image acquisition and processing

Microscopic data collection using SEM resulted in 12 sets of images describing blackcurrant powders (Figure 3a–l). Each variant stored information about the morphological structure of the microparticles (Figure 3).

Table 3: Results of blackcurrant powders using CNN

	Model	Precision	MSE (10–4)	MAE (10–4)	Val_accuracy	Val_mse (10–4)	Val_mae (10–4)	Val_precision	Recall	Accuracy	Val_recall
1	MD50-IN50	1.0000	0.0009	1.2020	1.0000	8.4583	39.0524	1.0000	1.0000	1.0000	1.0000
2	MD50-MD70	1.0000	0.0005	5,417	1.0000	2.5741	45.9237	1.0000	1.0000	1.0000	1.0000
3	GA50-GA70	0.9750	74.7065	184.1010	1.0000	16.1935	117.9243	0.9535	1.0000	1.0000	1.0000
4	W70-IN70	1.0000	0.6201	19	1.0000	0.217	5.4210	1.0000	1.0000	1.0000	1.0000
5	C70-W70	0.9778	73	186	1.0000	1.0196	16	1.0000	1.0000	0.9865	1.0000
6	F50-F70	1.0000	114	316	0.9688	193	360	0.9697	0.9394	0.9750	0.9697
7	F50-MD50	0.9875	130.6599	313.9229	0.9688	288.8454	434.4893	1.0000	0.9750	0.9697	0.9697
8	GA50-IN50	1.0000	14.3871	77.7426	0.9688	159.2872	343.5659	1.0000	1.0000	0.9429	1.0000
9	F50-G50	1.0000	0.0086	2.3117	0.9531	362.9437	517.1319	1.0000	1.0000	1.0000	0.9063
10	C50-GA50	1.0000	0.5910	25.0927	0.9531	338.3946	626.7399	1.0000	1.0000	0.9118	1.0000
11	IN50-IN70	0.9750	92.9790	334.8764	0.9531	431.1070	583.4963	0.9722	0.9722	1.0000	0.9063
12	F70-IN70	0.9767	177	452	0.9531	333	464.0000	0.9394	1.0000	0.9875	0.9688
13	F70-MD70	1.0000	23	92	0.9531	468	620.0000	0.9394	1.0000	1.0000	0.9688
14	MD50-W50	0.9875	67.1487	158.4006	0.9219	686.1994	1162.6472	0.9750	1.0000	1.0000	0.8333
15	MD50-GA50	1.0000	0.0523	4.0701	0.9063	593.6483	908.9045	1.0000	1.0000	1.0000	0.8125
16	W50-IN50	0.9865	85.0857	234.1973	0.8750	944.5102	1343.1749	0.9744	1.0000	0.7949	1.0000
17	W50-W70	1.0000	11.3038	149.9944	0.8438	1138.6122	1738.1969	1.0000	1.0000	1.0000	0.7059
18	C70-IN70	1.0000	33	189	0.8125	1480	2038	0.7209	1.0000	1.0000	1.0000
19	C50-MD50	0.9375	483.5656	806.4995	0.7813	1604.3843	2257.4732	1.0000	0.8611	0.7143	1.0000
20	F70-GA70	1.0000	155	411	0.7812	1716	2020	0.6818	0.9474	0.9750	1.0000
21	GA50-W50	1.0000	0.3772	12.8679	0.7344	2291.7201	2503.0488	1.0000	1.0000	0.6531	1.0000

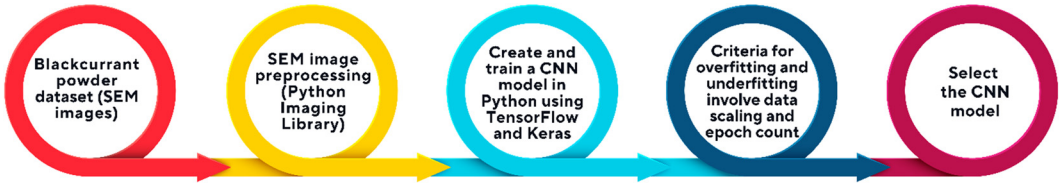

Figure 4: CNN procedure in blackcurrant powders: SEM image preparation, image preprocessing, creating CNN, tuning model CNN in training, and generate adequate CNN model.

3.4 Design and learning of convolutional networks

Under the designed CNN models and taking into account the criterion set in the methodology, *i.e.*, over-fitting by under-fitting analysis, and a fixed number of epochs equal to 100 during the learning of each CNN model, it was possible to obtain the results that are shown in Table 3. In Figure 4, the process of obtaining a CNN model is shown, according to the established standard for the design of ANN models in machine learning. Between the variants of blackcurrant powders for which the input data consisted of SEM images, *i.e.*, objects in the form of powder microparticles, the best identified were those with the highest proportion of carriers (50% content) for maltodextrin and inulin (MD50-IN50) (Figure 5a–c). The MD50-IN50 CNN model had the lowest mean square error (MSE) for the test set, which was 8.4583×10^{-4} (Figure 5b), respectively. In comparison, the weakest fit to the data of 50% content and type of carrier in blackcurrant powders was determined by the CNN GA50-W50 model, for which MSE = 2291.7201×10^{-4} (Table 3). Considering the results obtained, those models not included in Table 1 did not meet the criterion of over-fitting and under-fitting relationships, for which the value of the MSE coefficient determined a value above 0.22 and the accuracy coefficient below the fit value at 0.71.

3.4.1 Results of blackcurrant powders using CNN

In the case of results determining the proportion of carrier in the blackcurrant powder carrier variant, the best data recognition rate using the CNN model was achieved with the proportion of maltodextrin or gum arabic carrier. The CNN model (MD50-MD70) (Figure 5d–f) with the lowest proportion of maltodextrin carrier achieved a MSE value of 2.5741×10^{-4} (Figure 5e). In the case of the CNN model (GA50-GA70) (Figure 5g–i), for which the carrier was gum arabic the MSE for the test set was 16.1935×10^{-4} (Figure 5h). Considering the weakest result but at the same time meeting the criterion of CNN model fit was achieved with the CNN model (W50-W70) with the content of milk whey protein carrier.

Considering the type and the smallest proportion of the carrier (30% content) in blackcurrant powder, it turns out that the best CNN learning results were obtained with the participation of milk whey protein carriers with inulin and microcrystalline cellulose (W70-IN70, C70-W70), where the CNN models W70-IN70 (Figure 5j–l) and CNN C70-W70 (Figure 5m, n) achieved MSE values of, respectively, 0.0217 $\times 10^{-4}$ and 1.0196×10^{-4}. In comparison, the weakest result for identifying the 30% carrier share between powder variants was achieved by the CNN F70-GA70 model, where the MSE was $1{,}716 \times 10^{-4}$.

In Figure 4, it was illustrated the learning results for CNNs characterized by high accuracy, the lowest MSE, and mean absolute error (MAE) in the test set (val_mse, val_mae). The MSE and MAE values suggest that the CNN model predicts the output values well and minimizes discrepancies with the actual labels. Comparing the error functions for the training and test sets, it can be seen that the CNN model shows no clear signs of over-fitting, as confirmed by the stable difference between the errors in the two sets.

These results suggest that the CNN can be effectively used to identify fruit powders, and its accuracy and low error values make it a potentially useful tool in practical applications.

4 Discussion

As a result of the research using microscopic images (SEM), 21 out of 36 CNN models were selected (meeting the over-fitting by under-fitting criterion), which represented combinations with the smallest (30%) and largest (50%) proportion of the selected carrier type in the blackcurrant solution. Based on the results, it can be concluded that it is possible to identify blackcurrant powder microparticles using CNNs. Previous research efforts confirm the effectiveness of artificial intelligence in fruit powder identification [54]. Other studies have investigated the possibility of reducing the carrier content in the production of fruit powders using a spray drying method, with the aim of

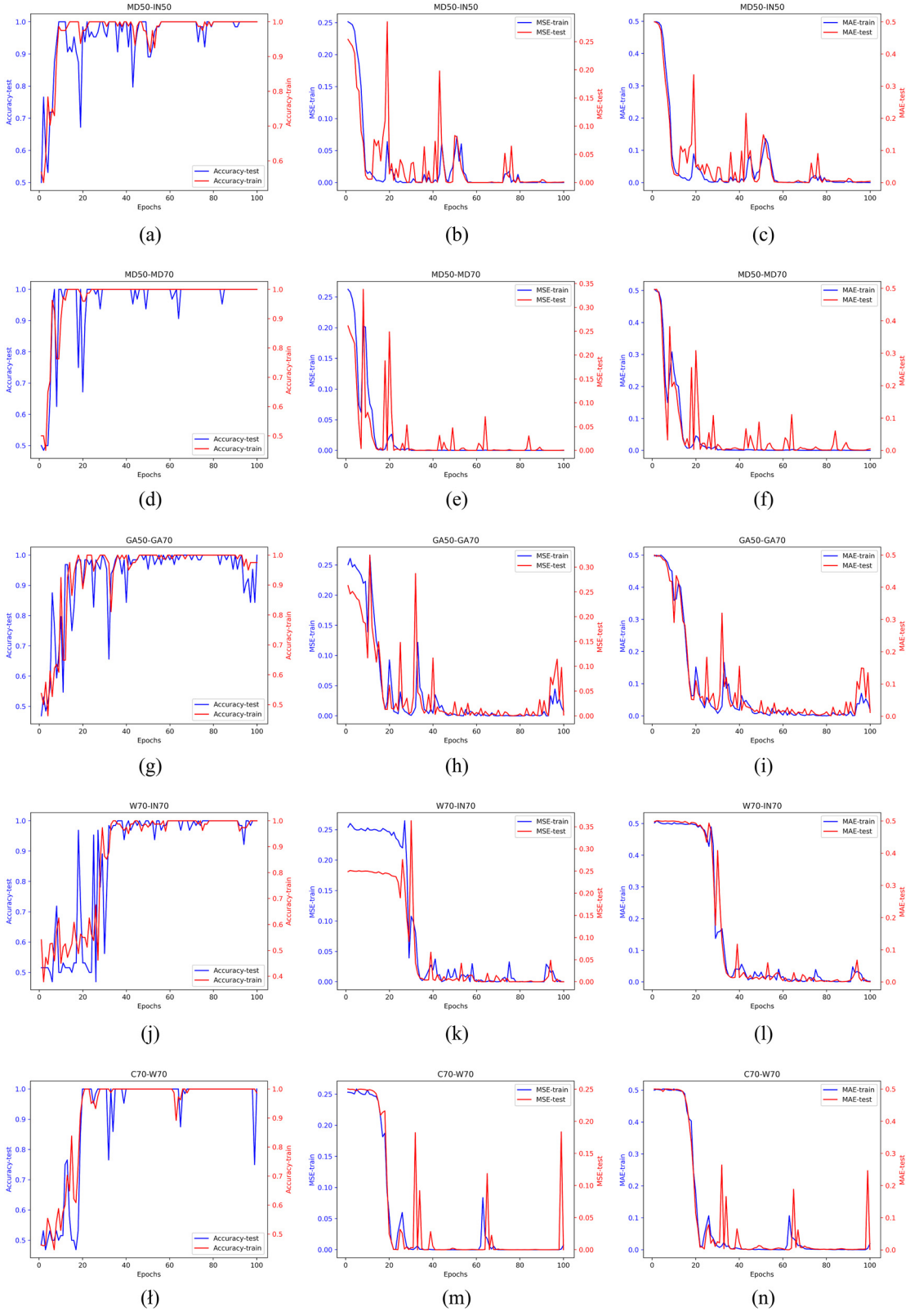

Figure 5: Learning charts (accuracy factor), MSE, and MAE for the five highest obtained results from the 21 respective CNNs: MD50-IN50 (a)–(c), MD50-MD70 (d)–(f), GA50-GA70 (g)–(i), W70-IN70 (j)–(l), C70-W70 (ł), (m), and (n).

obtaining fruit powders with a lower carrier content [15]. The current research compared the highest and lowest carrier contents in fruit powders. The aim of the endeavor became an attempt to prove that CNN's are as effective as possible in evaluating research variants with the lowest amount of carrier, for which the key aspect will be the ability to reduce energy costs in the manufacturing process of the final product. Other previous studies have taken into account that raspberry powders should be characterized by a regular shape of microparticles and contain the smallest possible intermolecular space [20]. In the current study results, the regular shape of these microparticles was also taken into account for comparison using LF-NMR and instrumental texture. Both in the previous studies and in the current one, the acquisition of a regular shape and an ordered interparticle structure is the key aspect in obtaining powders with a high quality index (homogeneity).

The current research examined how other carriers behave when extracting fruit powders. The focus was on the smallest and largest proportion of the carrier. As a result of the current and previous studies, it is confirmed that the recognition of regular microparticle shape and ordered intermolecular structure at 50% carrier content occurs with inulin and maltodextrin, among others [15]. When the ratio is reduced to 30% of the carrier content, it is confirmed to previous studies that identification of microparticle structure occurs best with inulin [12,20]. In the current study, milk whey proteins and microcrystalline cellulose were also successfully identified by CNN models as well as interpreted by textural parameters and the LF-NMR method.

In the study of texture analysis for the demonstrated carriers, statistically good solubility, hardness, cohesion, and viscosity of the obtained blackcurrant powders by spray drying are confirmed. At 30% carrier content in solution, maltodextrin and whey milk proteins determine the lowest Force_1 content underlying the linearity of the powders, as well as a longer T_1 relaxation time determining their homogeneity and microparticle ordering. In the case of 50% carrier in the blackcurrant solution, the lowest Force_1 content is determined for maltodextrin (MD50), inulin (IN50), milk whey protein (W50), and microstaline cellulose (C50). For comparison by the LF-NMR method, the shortest T_1 relaxation time was acquired by the C50 variant as one of the two blackcurrant powder variants (also F50). Evaluating the other textural parameters and discussing the results, it turns out that maltodextrin, inulin, milk whey proteins, and microcrystalline cellulose become quite effective carriers in determining the appropriate morphological structure.

A machine learning technique using computer vision has successfully determined which models have the highest quality index when recognizing the morphological structure of blackcurrant powders using image pixels. Conducting physical analyses using parameters such as texture, spin–lattice T_1 relaxation time using LF-NMR requires wider costs, more energy, and specialized training in their use. Therefore, it seems reasonable to use the latest artificial intelligence methods to assist in faster determination of the morphological structure of microparticles. CNNs were able to effectively identify the morphological structure of blackcurrant powders much faster and more efficiently than analytical methods. This translates into optimization of many unit processes in obtaining the final product. Machine learning is becoming an alternative solution to support the process of obtaining high-quality powders with desired properties. As a result of controlling the morphological structure of fruit powders, it becomes possible to optimize the spray drying process based on computer vision. Obtaining fruit powders with homogeneous microparticle shape and small inter-particle space in the spray drying process and evaluating them effectively using machine learning becomes a key criterion for maintaining the reproducibility of these results. This implies working on producing an intelligent powder obtaining system that controls the morphological structure of powders based on online computer vision.

5 Conclusions

In conclusion, according to the results obtained, it is possible to identify blackcurrant powder microparticles using CNNs and the Python language. The training CNNs gave the best results using carriers such as milk whey protein, inulin, and microcrystalline cellulose (designated W70-IN70 and C70-W70). The CNN models designated W70-IN70 and CNN C70-W70 achieved the lowest MSE values.

Currently, the aim is to improve a range of decision-making problems using advanced techniques by building machine learning models, data visualization, automation, and optimization of production processes using Python. Artificial intelligence is still evolving and the food industry can expect even further advances. Neural models can assist in reducing food waste, and AI-based robotics can revolutionize food processing and distribution. In the future, the experience will allow the implementation of online machine learning and deep learning solutions in the food industry as well. It is intended to implement convolutional network models in designing a homogeneous and ordered morphological structure of microparticles to obtain high-quality powders during spray drying (online). This will result in a final product with preserved nutritional values and their effective shelf life.

Funding information: The work was financially supported by a grant from the National Science Centre (Poland) No. 2021/05/X/NZ9/01014 (PI: Krzysztof Przybył). The publication was co-financed by the Polish Minister of Science and Higher Education as part of the Strategy of the Poznan University of Life Sciences for 2024–2026 in the field of improving scientific research and development work in priority research areas.

Author contributions: Conceptualization: Krzysztof Przybył; methodology: Krzysztof Przybył, Katarzyna Samborska, Hanna Maria Baranowska; software: Krzysztof Przybył; validation: Krzysztof Przybył; formal analysis: Krzysztof Przybył; investigation: Łukasz Masewicz, Aleksandra Jedlińska; resources: Krzysztof Przybył, Hanna Maria Baranowska, Przemysław Łukasz Kowalczewski; data curation: Krzysztof Przybył; writing – original draft preparation: Krzysztof Przybył; writing – review and editing: Krzysztof Przybył, Przemysław Łukasz Kowalczewski, Krzysztof Koszela, Katarzyna Samborska, Hanna Maria Baranowska, Łukasz Masewicz, Aleksandra Jedlińska; visualization: Krzysztof Przybył; supervision: Katarzyna Samborska, Hanna Maria Baranowska, Przemysław Łukasz Kowalczewski, Krzysztof Koszela. All authors have accepted responsibility for the entire content of this manuscript and approved its submission.

Conflict of interest: The authors state no conflict of interest.

Data availability statement: The data presented in this study are openly available in Repository for Open Data - RepOD at DOI: https://doi.org/10.18150/J6R7UY.

References

[1] Focker, M., E. D. van Asselt, B. J. A. Berendsen, M. G. M. van de Schans, S. P. J. van Leeuwen, S. M. Visser, et al. Review of food safety hazards in circular food systems in Europe. *Food Research International*, Vol. 158, 2022 Aug, id. 111505. https://linkinghub.elsevier.com/retrieve/pii/S0963996922005634.

[2] Iranshahi, K., D. I. Onwude, A. Martynenko, and T. Defraeye. Dehydration mechanisms in electrohydrodynamic drying of plant-based foods. *Food and Bioproducts Processing*, Vol. 131, 2022 Jan, pp. 202–216. https://linkinghub.elsevier.com/retrieve/pii/S0960308521001838.

[3] Richter Reis, F., C. Marques, A. C. S. Moraes, and M. L. de, Masson. Trends in quality assessment and drying methods used for fruits and vegetables. *Food Control*, Vol. 142, 2022 Dec, id. 109254. https://linkinghub.elsevier.com/retrieve/pii/S0956713522004479.

[4] Xu, X., Y. Lu, B. Vogel-Heuser, and L. Wang. Industry 4.0 and Industry 5.0—inception, conception and perception. *Journal of Manufacturing Systems*, Vol. 61, 2021 Oct, pp. 530–535. https://linkinghub.elsevier.com/retrieve/pii/S0278612521002119.

[5] Lingayat, A. B., V. P. Chandramohan, V. R. K. Raju, and V. Meda. A review on indirect type solar dryers for agricultural crops – dryer setup, its performance, energy storage and important highlights. *Applied Energy*, Vol. 258, 2020 Jan, id. 114005. https://linkinghub.elsevier.com/retrieve/pii/S0306261919316927.

[6] Raponi, F., R. Moscetti, D. Monarca, A. Colantoni, and R. Massantini. Monitoring and optimization of the process of drying fruits and vegetables using computer vision: a review. *Sustainability*, Vol. 9, No. 11, 2017 Nov, id. 2009. https://www.mdpi.com/2071-1050/9/11/2009.

[7] Gill, H. S., G. Murugesan, A. Mehbodniya, G. Sekhar Sajja, G. Gupta, and A. Bhatt. Fruit type classification using deep learning and feature fusion. *Computers and Electronics in Agriculture*, Vol. 211, 2023 Aug, id. 107990. https://linkinghub.elsevier.com/retrieve/pii/S0168169923003782.

[8] Massaro, A. Advanced control systems in industry 5.0 enabling process mining. *Sensors*, Vol. 22, No. 22, 2022 Nov, id. 8677. https://www.mdpi.com/1424-8220/22/22/8677.

[9] Min, W., Z. Wang, J. Yang, C. Liu, and S. Jiang. Vision-based fruit recognition via multi-scale attention CNN. *Computers and Electronics in Agriculture*, Vol. 210, 2023 Jul, id. 107911. https://linkinghub.elsevier.com/retrieve/pii/S0168169923002995.

[10] Zheng, M., S. Zhang, Y. Zhang, and B. Hu. Construct food safety traceability system for people's health under the internet of things and big data. *IEEE Access*, Vol. 9, 2021, pp. 70571–70583. https://ieeexplore.ieee.org/document/9427143/.

[11] Boobier, T. *Advanced analytics and AI: impact, implementation, and the future of work*, John Wiley & Sons, Ltd, Hoboken, New Jersey, USA, 2018.

[12] Przybył, K. and K. Koszela. Applications MLP and other methods in artificial intelligence of fruit and vegetable in convective and spray drying. *Applied Sciences*, Vol. 13, No. 5, 2023 Feb, id. 2965. https://www.mdpi.com/2076-3417/13/5/2965.

[13] Sun, Q., M. Zhang, and A. S. Mujumdar. Recent developments of artificial intelligence in drying of fresh food: a review. *Critical Reviews in Food Science and Nutrition*, Vol. 59, No. 14, 2019 Aug, pp. 2258–2275. https://www.tandfonline.com/doi/full/10.1080/10408398.2018.1446900.

[14] Jedlińska, A., K. Samborska, A. Wiktor, M. Balik, D. Derewiaka, A. Matwijczuk, et al. Spray drying of pure kiwiberry pulp in dehumidified air. *Drying Technology*, Vol. 40, No. 7, 2022 Jun, pp. 1421–1435. https://www.tandfonline.com/doi/full/10.1080/07373937.2020.1871006.

[15] Przybył, K., K. Koszela, F. Adamski, K. Samborska, K. Walkowiak, and M. Polarczyk. Deep and machine learning using SEM, FTIR, and texture analysis to detect polysaccharide in raspberry powders. *Sensors*, Vol. 21, No. 17, 2021 Aug, id. 5823. https://www.mdpi.com/1424-8220/21/17/5823.

[16] Samborska, K., A. Jedlińska, A. Wiktor, D. Derewiaka, R. Wołosiak, A. Matwijczuk, et al. The effect of low-temperature spray drying with dehumidified air on phenolic compounds, antioxidant activity, and aroma compounds of rapeseed honey powders. *Food and Bioprocess Technology*, Vol. 12, No. 6, 2019 Jun, pp. 919–932. http://link.springer.com/10.1007/s11947-019-02260-8.

[17] Feguš, U., U. Žigon, M. Petermann, and Ž. Knez. Effect of drying parameters on physiochemical and sensory properties of fruit

powders processed by PGSS-, vacuum- and spray-drying. *Acta Chimica Slovenica*, Vol. 62, No. 2, 2015 Jun, pp. 479–487. https://journals.matheo.si/index.php/ACSi/article/view/969.

[18] Santos, D., A. C. Maurício, V. Sencadas, J. D. Santos, M. H. Fernandes, and P. S. Gomes. Spray drying: an overview. In *Biomaterials – physics and chemistry – New Edition*, InTech, London, UK, 2018. http://www.intechopen.com/books/biomaterials-physics-and-chemistry-new-edition/spray-drying-an-overview.

[19] Shishir, M. R. I. and W. Chen. Trends of spray drying: a critical review on drying of fruit and vegetable juices. *Trends in Food Science and Technology*, Vol. 65, 2017 Jul, pp. 49–67. https://linkinghub.elsevier.com/retrieve/pii/S0924224416306355.

[20] Przybył, K., K. Samborska, K. Koszela, L. Masewicz, and T. Pawlak. Artificial neural networks in the evaluation of the influence of the type and content of carrier on selected quality parameters of spray dried raspberry powders. *Measurement*, Vol. 186, 2021 Dec, id. 110014. https://linkinghub.elsevier.com/retrieve/pii/S0263224121009416.

[21] Jeżowski, P., J. Menzel, H. M. Baranowska, and P. Ł. Kowalczewski. Microwaved-assisted synthesis of starch-based biopolymer membranes for novel green electrochemical energy storage devices. *Materials (Basel)*, Vol. 16, No. 22, 2023 Nov, id. 7111. https://www.mdpi.com/1996-1944/16/22/7111.

[22] Luo, J., M. Li, Y. Zhang, M. Zheng, and C. Ming Ling. The low-field NMR studies the change in cellular water in tilapia fillet tissue during different drying conditions. *Food Science & Nutrition*, Vol. 9, No. 5, 2021 May, pp. 2644–2657. https://onlinelibrary.wiley.com/doi/10.1002/fsn3.2221.

[23] Nestle, N. NMR relaxometry study of cement hydration in the presence of different oxidic fine fraction materials. *Solid State Nuclear Magnetic Resonance*, Vol. 25, No. 1–3, 2004 Jan, pp. 80–83. https://linkinghub.elsevier.com/retrieve/pii/S0926204003000870.

[24] Walkowiak, K., K. Przybył, H. M. Baranowska, K. Koszela, Ł. Masewicz, and M. Piątek. The process of pasting and gelling modified potato starch with LF-NMR. *Polymers (Basel)*, Vol. 14, No. 1, 2022 Jan, id. 184, https://www.mdpi.com/2073-4360/14/1/184.

[25] Mao, Y., H. Li, Y. Wang, H. Wang, J. Shen, Y. Xu, et al. Rapid monitoring of tea plants under cold stress based on UAV multi-sensor data. *Computers and Electronics in Agriculture*, Vol. 213, 2023 Oct, id. 108176. https://linkinghub.elsevier.com/retrieve/pii/S0168169923005641.

[26] Sejnowski, T. J. *The deep learning revolution*, The MIT Press, Cambridge, MA, USA, 2018.

[27] Bremser, W. NMR macht Spaß! Experimental pulse NMR: a nuts and bolts approach. Von E. Fukushima/S. B. W. Roeder. Addison-Wesley Publishing Company Inc. Reading, MA-London-Amsterdam-Don Mills-Ontario-Sydney-Tokyo 1981. XIV, 539 S., geb., $34,50. Nachrichten aus Chemie, *Technik und Laboratorium*, Vol. 30, No. 2, 1982 Feb, id. 144. https://onlinelibrary.wiley.com/doi/10.1002/nadc.19820300213.

[28] Fukushima, E. and S. B. W. Roeder. *Experimental pulse NMR*, CRC Press, Boca Raton, Florida, USA, 2018. https://www.taylorfrancis.com/books/9780429962417.

[29] Węglarz, W. P. and H. Harańczyk. Two-dimensional analysis of the nuclear relaxation function in the time domain: the program CracSpin. *Journal of Physics D: Applied Physics*, Vol. 33, No. 15, 2000 Aug, pp. 1909–1920. http://stacks.iop.org/0022-3727/33/i=15/a=322?key=crossref.d9297399fd9aa25ff88d352dfa89b19b.

[30] Lawless, C., D. J. Wilkinson, A. Young, S. G. Addinall, and D. A. Lydall. Colonyzer: automated quantification of micro-organism growth characteristics on solid agar. *BMC Bioinformatics*, Vol. 11, No. 1, 2010 Dec, id. 287. https://bmcbioinformatics.biomedcentral.com/articles/10.1186/1471-2105-11-287.

[31] Guo, X., Y. Ge, F. Liu, and J. Yang. Identification of maize and wheat seedlings and weeds based on deep learning. *Frontiers in Earth Science*, Vol. 11, 2023 Feb, id. 1146558. https://www.frontiersin.org/articles/10.3389/feart.2023.1146558/full.

[32] Krizhevsky, A., I. Sutskever, and G. E. Hinton. ImageNet classification with deep convolutional neural networks. *Communications of the ACM*, Vol. 60, No. 6, 2017 May, pp. 84–90. https://dl.acm.org/doi/10.1145/3065386.

[33] Rauf, H. T., M. I. U. Lali, S. Zahoor, S. Z. H. Shah, A. U. Rehman, and S. A. C. Bukhari. Visual features based automated identification of fish species using deep convolutional neural networks. *Computers and Electronics in Agriculture*, Vol. 167, 2019 Dec, id. 105075. https://linkinghub.elsevier.com/retrieve/pii/S0168169919313523.

[34] Chollet, F. *Deep learning with python*, Manning Publications Co., Cham, Switzerland, 2017.

[35] Yang, J. and G. Yang. Modified convolutional neural network based on dropout and the stochastic gradient descent optimizer. *Algorithms*, Vol. 11, No. 3, 2018 Mar, id. 28. https://www.mdpi.com/1999-4893/11/3/28.

[36] Kingma, D. P. and J. Ba. *Adam: a method for stochastic optimization*, 2017 Jan. http://arxiv.org/abs/1412.6980.

[37] Zou, F., L. Shen, Z. Jie, W. Zhang, and W. Liu. A sufficient condition for convergences of adam and RMSProp. In *2019 IEEE/CVF Conference on Computer Vision and Pattern Recognition (CVPR)*, IEEE, 2019, pp. 11119–11127. https://ieeexplore.ieee.org/document/8954145/.

[38] Ogundokun, R. O., R. Maskeliunas, S. Misra, and R. Damaševičius. Improved CNN based on batch normalization and adam optimizer. In: *Computational Science and Its Applications – ICCSA 2022 Workshops. ICCSA 2022. Lecture Notes in Computer Science*, Vol. 13381, Springer, Cham, 2022, pp. 593–604. https://doi.org/10.1007/978-3-031-10548-7_43.

[39] Bashir, D., G. D. Montañez, S. Sehra, P. S. Segura, and J. Lauw. An information-theoretic perspective on overfitting and underfitting. In: *AI 2020: Advances in Artificial Intelligence, AI 2020, Lecture Notes in Computer Science*, Vol 12576. Springer, Cham, 2020, pp. 347–358. https://doi.org/10.1007/978-3-030-64984-5_27.

[40] Kuti, T., A. Hegyi, and S. Kemény. Analysis of sensory data of different food products by ANOVA. *Chemometrics and Intelligent Laboratory Systems*, Vol. 72, No. 2, 2004 Jul, pp. 253–257. https://linkinghub.elsevier.com/retrieve/pii/S0169743904000437.

[41] Rust, A., F. Marini, M. Allsopp, P. J. Williams, and M. Manley. Application of ANOVA-simultaneous component analysis to quantify and characterise effects of age, temperature, syrup adulteration and irradiation on near-infrared (NIR) spectral data of honey. *Spectrochimica Acta Part A: Molecular and Biomolecular Spectroscopy*, Vol. 253, 2021 May, id. 119546, https://linkinghub.elsevier.com/retrieve/pii/S1386142521001220.

[42] Guo, Y., Y. Zhou, and Z. Zhang. Fault diagnosis of multi-channel data by the CNN with the multilinear principal component analysis. *Measurement*, Vol. 171, 2021 Feb, id. 108513, https://linkinghub.elsevier.com/retrieve/pii/S026322412031040X.

[43] Ahmad, S., I. Pasha, M. Saeed, and M. Shahid. Principal component analysis and correlation studies of spring wheats in relation to cookie making quality. *International Journal of Food Properties*, Vol. 20, No. 10, 2017 Oct, pp. 2299–2313. https://www.tandfonline.com/doi/full/10.1080/10942912.2016.1236273.

[44] Jolliffe, I. T. *Principal component analysis*, Springer-Verlag, New York, 2002. (Springer Series in Statistics). http://link.springer.com/10.1007/b98835.

[45] Flowers, B., K.-T. Huang, and G. O. Aldana. Analysis of the habitat fragmentation of ecosystems in belize using landscape metrics. *Sustainability*, Vol. 12, No. 7, 2020 Apr, id. 3024. https://www.mdpi.com/2071-1050/12/7/3024.

[46] Sudha Mishra, S. and A. K. Das Mohapatra. Weavers' perception towards sustainability of Sambalpuri handloom: a Tukey's HSD test analysis. *Materials Today: Proceedings*, Vol. 51, 2022, pp. 217–227. https://linkinghub.elsevier.com/retrieve/pii/S2214785321038335.

[47] Frochte, J. Python, NumPy, SciPy und Matplotlib – in a nutshell. In *Maschinelles Lernen*, Carl Hanser Verlag GmbH & Co. KG, München, 2020, pp. 38–77. https://www.hanser-elibrary.com/doi/10.3139/9783446463554.003.

[48] van der Walt, S., J. L. Schönberger, J. Nunez-Iglesias, F. Boulogne, J. D. Warner, N. Yager, et al. Scikit-image: image processing in Python. *PeerJ*, Vol. 2, 2014 Jun, id. e453. https://peerj.com/articles/453.

[49] Di Monaco, R., S. Cavella, and P. Masi. Predicting sensory cohesiveness, hardness and springiness of solid foods from instrumental measurements. *Journal of Texture Studies*, Vol. 39, No. 2, 2008 Apr, pp. 129–149. https://onlinelibrary.wiley.com/doi/10.1111/j.1745-4603.2008.00134.x.

[50] Rosenthal, A. J. and P. Thompson. What is cohesiveness? A linguistic exploration of the food texture testing literature. *Journal of Texture Studies*, Vol. 52, No. 3, 2021 Jun, pp. 294–302. https://onlinelibrary.wiley.com/doi/10.1111/jtxs.12586.

[51] Tobin, A. B., P. Heunemann, J. Wemmer, J. R. Stokes, T. Nicholson, E. J. Windhab, et al. Cohesiveness and flowability of particulated solid and semi-solid food systems. *Food & Function*, Vol. 8, No. 10, 2017, pp. 3647–3653. https://xlink.rsc.org/?DOI=C7FO00715A.

[52] Lim, H. L., K. P. Hapgood, and B. Haig. Understanding and preventing agglomeration in a filter drying process. *Powder Technology*, Vol. 300, 2016 Oct, pp. 146–156. https://linkinghub.elsevier.com/retrieve/pii/S0032591016300961.

[53] Różańska, M. B., J. Zembrzuska, P. Rychlewski, M. Kidoń, Ł. Masewicz, S. Mildner-Szkudlarz, et al. Exploring the impact of dietary fiber enrichment on molecular water properties and indicators of Maillard reaction (furosine, Nε-carboxymethyllysine, and Nε-carboxyethyllysine) in model gluten-free bread. *Food Chemistry*, Vol. 491, 2025 Nov, id. 145194. https://linkinghub.elsevier.com/retrieve/pii/S0308814625024458.

[54] Przybył, K., J. Gawałek, K. Koszela, J. Wawrzyniak, and L. Gierz. Artificial neural networks and electron microscopy to evaluate the quality of fruit and vegetable spray-dried powders. Case study: strawberry powder. *Computers and Electronics in Agriculture*, Vol. 155, 2018 Dec, pp. 314–323. https://linkinghub.elsevier.com/retrieve/pii/S0168169918303466.